Mathematical projections of air pollutants effects over Niger Delta region using remotely sensed satellite data

3 authors, including:

Temidayo Omotosho
Covenant University Ota Ogun State, Nigeria

39 PUBLICATIONS   **111** CITATIONS

Some of the authors of this publication are also working on these related projects:

Project   Aerosol Dispersion in West Africa and its implcation on climate change. View project

Project   RENEWABLE ENERGY PROSPECTS IN DEVELOPING COUNTRIES View project

Mathematical Projections of Air Pollutants Effects over Niger Delta Region Using Remotely Sensed Satellite Data

Omotosho T.V., Moses E. Emetere*, Arase O.S.

Department of Physics, Covenant University Canaan land,
P.M.B 1023, Ota, Nigeria.
*moses.emetere@covenantuniversity.edu.ng

Abstract

Air pollution due gas–flaring is a major concern in the Niger-Delta region of Nigeria. The short and long term effect of the massive air pollution on the life form within the area requires urgent attention because of the health implication. This research examines the impact of air pollutants in Niger-Delta region using remotely sensed satellite data. The satellite data set was obtained from CALIPSO, MODIS and ARIS. A mathematical software (MATLAB) was used to analyse the results. For Sulphur dioxide (SO_2) Uyo had the highest rate of pollution (0.67DU), then Yenegoa (0.66DU), Benin (0.64DU), Asaba (0.60DU), Port Harcourt (0.58DU), Calabar (0.55DU) respectively. For Carbon dioxide (CO_2), Yenegoa was the most polluted with (382.01ppmv), Port Harcourt, Calabar and Uyo all had (381.99ppmv) then Benin (381.77ppmv) and Asaba (381.53ppmv) respectively. For Nitrogen dioxide (NO_2), Port Harcourt had the highest mean value with ($54.65 mol/cm^2$), Asaba ($51.05 mol/cm^2$), Uyo ($49.08 mol/cm^2$),Calabar ($47.84 mol/cm^2$), Yenagoa ($46.73 mol/cm^2$), Benin ($43.22 mol/cm^2$) respectively. For Methane (CH_4), the stations with the highest rate of pollution were Port Harcourt, Yenagoa and Uyo with ($3.86E+19 mol/cm^2$), Benin and Asaba had ($3.8E+19 mol/cm^2$) while Calabar ($3.76E+19 mol/cm^2$). Mathematical projections were made to capture the dilemma- people in this region might encounter in the nearest future.

Keyword: gas flaring, mathematical model, aerosols, Niger-Delta region, green house gases, aerosol, sulphate, methane, carbon dioxide, nitrate oxide

1 Introduction

Gas-flaring emissions like other kind of anthropogenic emissions contribute

significantly to global warming, climate change and health deterioration of life-forms if not controlled [1-3]. Gas flares are composed of green gases and aerosols such as sulfur dioxide, oxides of carbon i.e. CO or CO_2, nitrogen dioxides, methane, benzapryene, toluene, xylene, and hydrogen sulfide. Unarguably, the steady emission of gas flares into the Niger-Delta region for the past thirty years should attract high volume of pollutants in the planetary boundary layer. Although this initiates unstable precipitations, the possibility of acidic or basic rainfall within the region is inevitable [4]. Aside gas flaring, there are other forms of pollutions which are categorized as point source or non point source pollution. However, the rigour of estimating the type of gases ejected and the locations the gases were ejected is difficulties that cannot be done via ground-truth. However, the remote sensing option is a better option to capture the amount of gas flares ejected into the atmosphere per time. The satellite data used for this research were generated from the Giovanni NASA satellite database, Giovanni is a tool that displays Earth science data from NASA satellites directly on the Internet. Giovanni is an acronym for the Goddard Earth Sciences Data and Information Services Center, or GES DISC, Interactive Online Visualization and Analysis Infrastructure. Various data can be generated on Giovanni i.e. atmospheric chemistry, atmospheric temperature, water vapor and clouds, atmospheric aerosols, precipitation, and ocean chlorophyll, surface temperature e.t.c. Basic analytical functions performed by Giovanni currently are carried out by the Grid Analysis and Display System (GrADS). Giovanni supports multiple data formats including Hierarchical Data Format (HDF), HDF-EOS, network Common Data Form (netCDF), GRIdded Binary (GRIB), and binary, and multiple plot types including area, time, Hovmoller, and image animation [5]. Many researchers have done the statistical analysis of air pollution of Niger-Delta [6-7]. The results obtained are not different from what is already known. Therefore, the need for a comprehensive mathematical model is essential for both predictive and proactive study of air pollution within the Niger-Delta. 'A model is not only a substitute of the actual system, it also the simplification of the system' [8]. A plume model can be any of the following, physical static model, physical dynamic model, mathematical static model, mathematical dynamic model, mathematical static analytical model, mathematical dynamic numerical model e.t.c. In this paper we analyze the results obtained from the Niger-Delta region and relate it to a dispersive semi plume model.

2 Theoretical Derivations

The Niger Delta region is described in figure (1) below. The number of oil exploration point-contributing to gas flaring cannot be ascertained for security reasons, However, we made few reasonable assumptions to suffice for the likely errors during the formulation of the model.
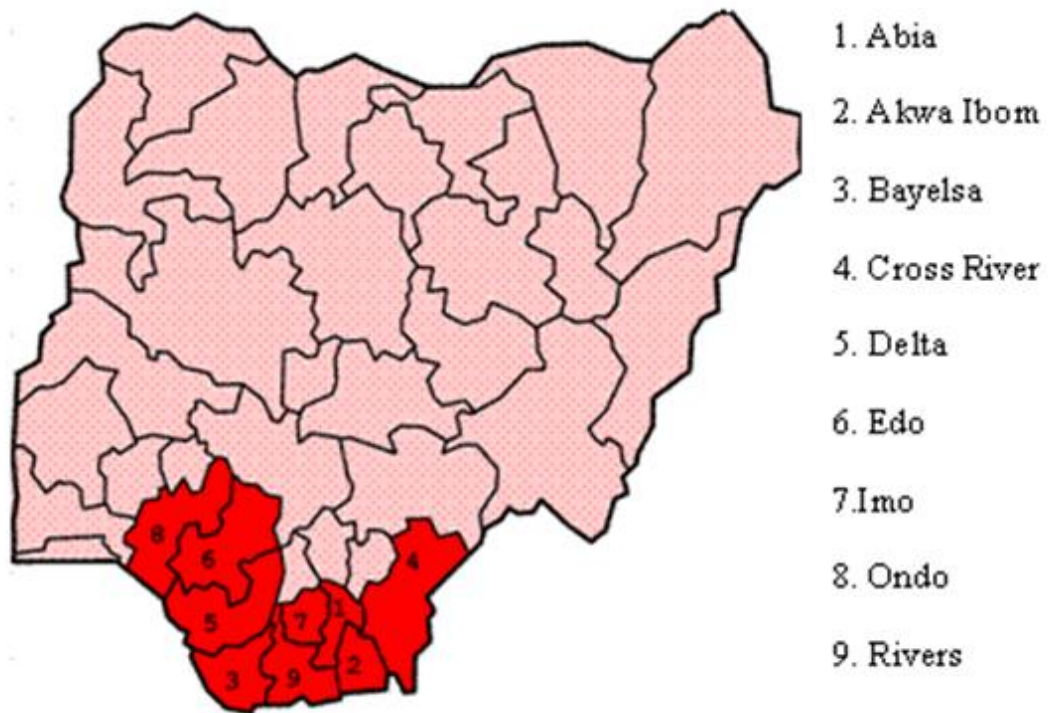
1. Abia
2. Akwa Ibom
3. Bayelsa
4. Cross River
5. Delta
6. Edo
7. Imo
8. Ondo
9. Rivers

Figure 1: Niger-Delta region at its constituents states. (http://en.wikipedia.org/wiki/Niger_Delta)

The graphics of the flare dispersion technique is highlighted in figure (2A-C) shown below.

Figure 2A-C: Types of gas flare dispersion. (http://www.foe.org/gas-flaring-nigeria)

Figure 2A is the vertical dispersion method, figure 2B is the scattered dispersion method and figure 2C is the horizontal dispersion method. The full analysis of all the methods had been established [1,2]. The following assumptions were adopted.

1. Inclusion of the mild diffusion at the downwind plane as shown in figure 2A-C. Therefore the measurement of the eddy diffusivity is between 2 -3 m^2/s, though it varies from place to place.
2. The angle of deviation (α & β) depends on the wind convection and it does not exceeds the angles. Therefore the gas flares noticed around the stack is as a result of the particulate gas flare splash from the lower turbulent diffusion as shown in figure (3)
3. The presence of air upthrust and air viscosity was made negligible because of the influence of the ground heat flux [9-10].
4. The width of the plume depends on both the wind direction and coefficient of eddy diffusivity.
5. The gas flare particulate is uniformly distributed along the sampling site.
6. The wind speed ranges $1ms^{-1}$ and $0.72ms^{-1}$ at 10m above the ground (below the planetary boundary layer) during the dry and wet seasons respectively

The pictorial view of particulate dispersion (figure 3) served as the control guide for this model. The model incorporates four equations i.e. general dispersion equation, mild dispersion equation, turbulent dispersion equation and particulate deposition equation. The mild dispersion equation and turbulent dispersion equation applies to any dispersion methods. However, the mild dispersion model is considered in this study because it solves the tropospheric gas transport [1]. Air particles at the mild dispersion region is the lightest by mass and energetic to interact with atmospheric current [11,12].
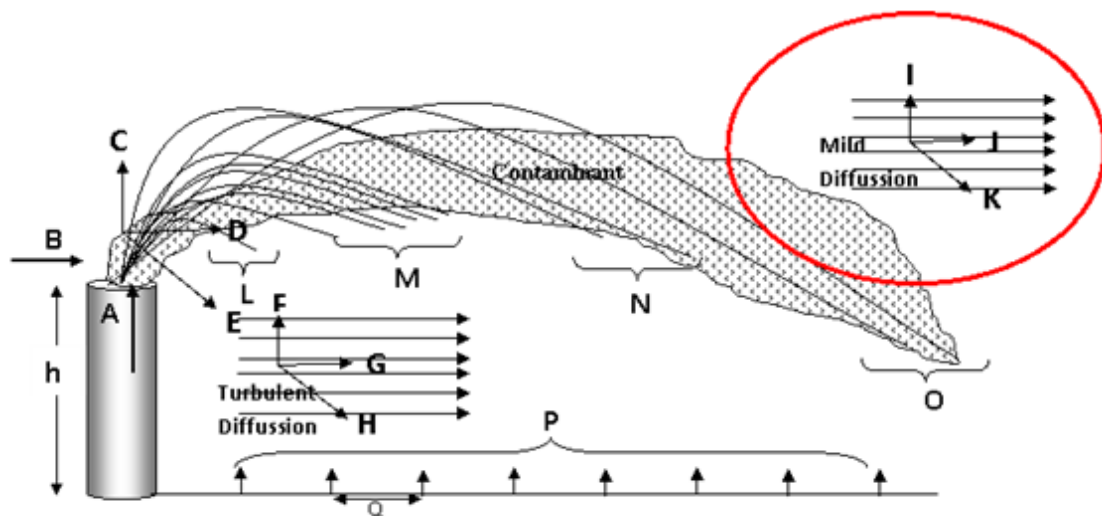

Figure 3: Pictorial analysis of the general dispersion model

Figure (3) expresses the different perspectives of the advection diffusion equations adopted for this model was derived. The mathematical expressions for the different positions are mathematically represented below.

Region **A-E** is the general particulate dispersion analysis

$$A = \frac{\partial c}{\partial t} \; ; B = V \frac{\partial c}{\partial r} \; ; C = V_z \frac{\partial c}{\partial z} \; ; D = V_x \frac{\partial c}{\partial x} \; ; E = V_y \frac{\partial c}{\partial y} \Big\} \tag{1}$$

Where $V^2 = V_x{}^2 + V_y{}^2 + V_z{}^2$

Region **F-H** is the turbulent particulate dispersion analysis

$$F = \frac{\partial}{\partial z}\left(K_z \frac{\partial c}{\partial z}\right); G = \frac{\partial}{\partial x}\left(K_z \frac{\partial c}{\partial x}\right) = 0 \; ; H = \frac{\partial}{\partial y}\left(K_y \frac{\partial c}{\partial y}\right) \tag{2}$$

Region **I-K** is the mild particulate dispersion analysis

$$I = \frac{\partial}{\partial z}\left(K_{z2} \frac{\partial c}{\partial z}\right); = \frac{\partial}{\partial x}\left(K_{z2} \frac{\partial c}{\partial x}\right) = 0 \; ; K = \frac{\partial}{\partial y}\left(K_{y2} \frac{\partial c}{\partial y}\right); \tag{3}$$

Region **L-O** is the particulate deposition analysis

$$L \approx \frac{2V_{1x}^3 V_y}{gV^2} \; ; M \approx \frac{2V_{2x}^3 V_y}{gV^2} \; ; \approx \frac{2V_{3x}^3 V_y}{gV^2} \; ; O \approx \frac{2V_{4x}^3 V_y}{gV^2} \Big\} \tag{4}$$

V is the wind velocity (m/s), P is the Air Upthrust, C (x,y,z) is the mean concentration of diffusing pollutants of diffusing substance at a point (x,y,z) [kg/m^3], Ky, Kx is the eddy diffusivities in the direction of the y- and z- axes [m^2/s] and S is the source/sink term [kg/m^3-s]

The governing equations are written as

$$\frac{\partial c}{\partial t} + V_x \frac{\partial c}{\partial x} - V_z \frac{\partial c}{\partial z} - V_y \frac{\partial c}{\partial y} = \frac{\partial}{\partial z}\left(K_z \frac{\partial c}{\partial z}\right) + \frac{\partial}{\partial y}\left(K_y \frac{\partial c}{\partial y}\right) + \frac{\partial}{\partial z}\left(K_{z2} \frac{\partial c}{\partial z}\right) + \frac{\partial}{\partial y}\left(K_{y2} \frac{\partial c}{\partial y}\right) - P + S \tag{5}$$

$$V_z \frac{\partial c}{\partial z} = \frac{\partial}{\partial z}\left(K_z \frac{\partial c}{\partial z}\right) + \frac{\partial}{\partial y}\left(K_y \frac{\partial c}{\partial y}\right) + \frac{\partial}{\partial x}\left(K_z \frac{\partial c}{\partial x}\right) \tag{6}$$

$$V_x \frac{\partial c}{\partial x} = \frac{\partial}{\partial y}\left(K_{y2} \frac{\partial c}{\partial y}\right) + \frac{\partial}{\partial z}\left(K_{z2} \frac{\partial c}{\partial z}\right) + \frac{\partial}{\partial x}\left(K_{z2} \frac{\partial c}{\partial x}\right) \tag{7}$$

Equation (7) is the mild dispersion equation. The mild dispersion equation occurs in two 2D on the account of individual gas molecule transport. It is mathematically expressed as

$$V_x \frac{\partial C_1}{\partial x} = \frac{\partial}{\partial y}\left(K_{y2}\frac{\partial C}{\partial y}\right) + \frac{\partial}{\partial z}\left(K_{z2}\frac{\partial C}{\partial z}\right)\Bigg\}$$
$$V_x \frac{\partial C_2}{\partial x} = \frac{\partial}{\partial z}\left(K_{z2}\frac{\partial C}{\partial z}\right) + \frac{\partial}{\partial x}\left(K_{z2}\frac{\partial C}{\partial x}\right)\Bigg\}$$

(8)

Equation (8) is the ascending particulate-mild dispersion equation

$$V_x \frac{\partial C_1}{\partial x} = \frac{\partial}{\partial y}\left(K_{y2}\frac{\partial C}{\partial y}\right) - \frac{\partial}{\partial z}\left(K_{z2}\frac{\partial C}{\partial z}\right)\Bigg\}$$
$$V_x \frac{\partial C_2}{\partial x} = -\frac{\partial}{\partial z}\left(K_{z2}\frac{\partial C}{\partial z}\right) + \frac{\partial}{\partial x}\left(K_{z2}\frac{\partial C}{\partial x}\right)\Bigg\}$$

(9)

Equation (9) is the descending particulate-mild dispersion equation
It was solved using separation of variable i.e. C=X (x)Y (y) with the initial boundary condition are x=1, X=1; y=1, Y=1; z=1, Z=1. The solution is given as

$$C\ (x,y,z) = a^2 b\cos\left(\frac{n}{k_y} + \alpha\right)\cos\left(\frac{n}{k_z} + \beta\right)\exp\left(\frac{n^2}{V_x}\right)$$

(10)

$a,\ b,\ n,$ α, and β are constants that would be determined via remotely sensed data set. The practical application of equation (10) is explained in the next session.
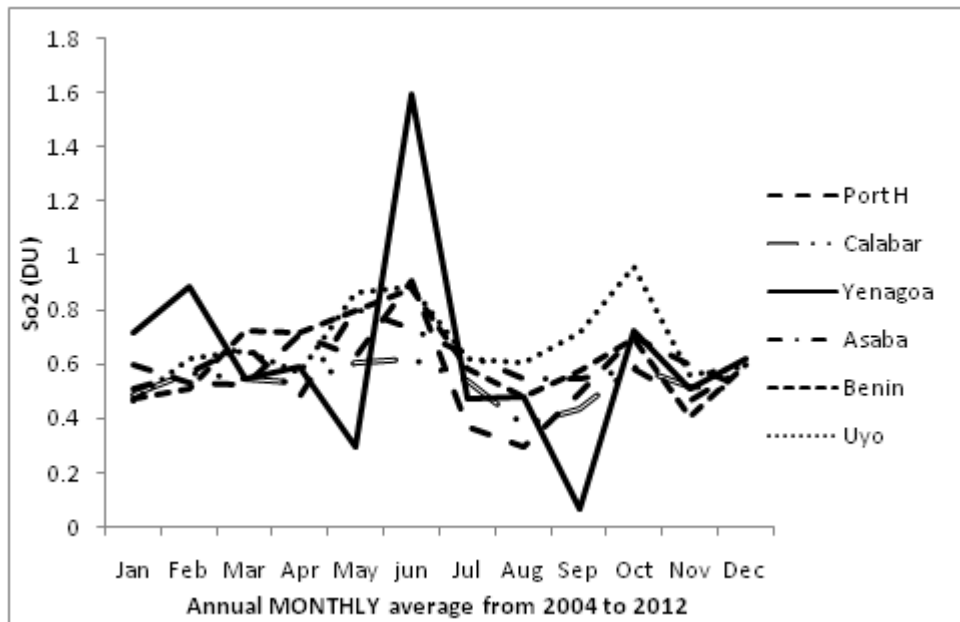

3   Results and Discussion

Figure 4: SO$_2$ satellite analysis from 2004 to 2012

Equations shown beside figure:

$$\frac{u^2}{V_x} = -0.005$$

$$\alpha = 0.05$$

$$\beta = 0.34$$

$$\frac{u}{k_{y_{max}}} = \frac{5}{4}\pi$$

$$\frac{u}{k_{z_{max}}} = -\frac{14}{4}\pi$$

$$\frac{u}{k_{y_{min}}} = \frac{3}{2}\pi$$

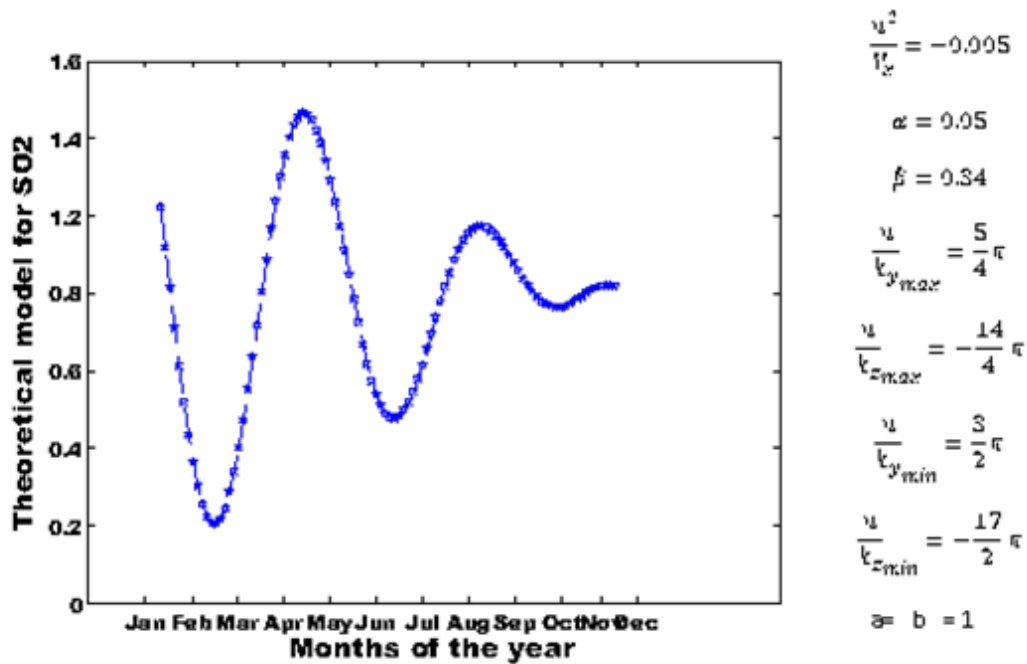$$\frac{u}{k_{z_{min}}} = -\frac{17}{2}\pi$$

$$a = b = 1$$

Figure 5: Theoretical model describing the SO₂ pattern and corresponding constants

In January and February it was obvious that the station that was mostly polluted by SO$_2$ was Yenegoa, followed by Port Harcourt then, by Asaba and then Calabar and after which we have Uyo and then the least polluted was Benin. Then in march and April it started to decrease in Yenagoa and increased in Benin, Asaba and then in May it took a drastic drop in Yenegoa and then picked up again in June to a maximum point of 1.6 DU while it decreased in the other stations in July and August then Yenegoa also took a huge drop in September and October while in Uyo we had a drastic increase while they just maintain a medium pollution level through October, November and December.
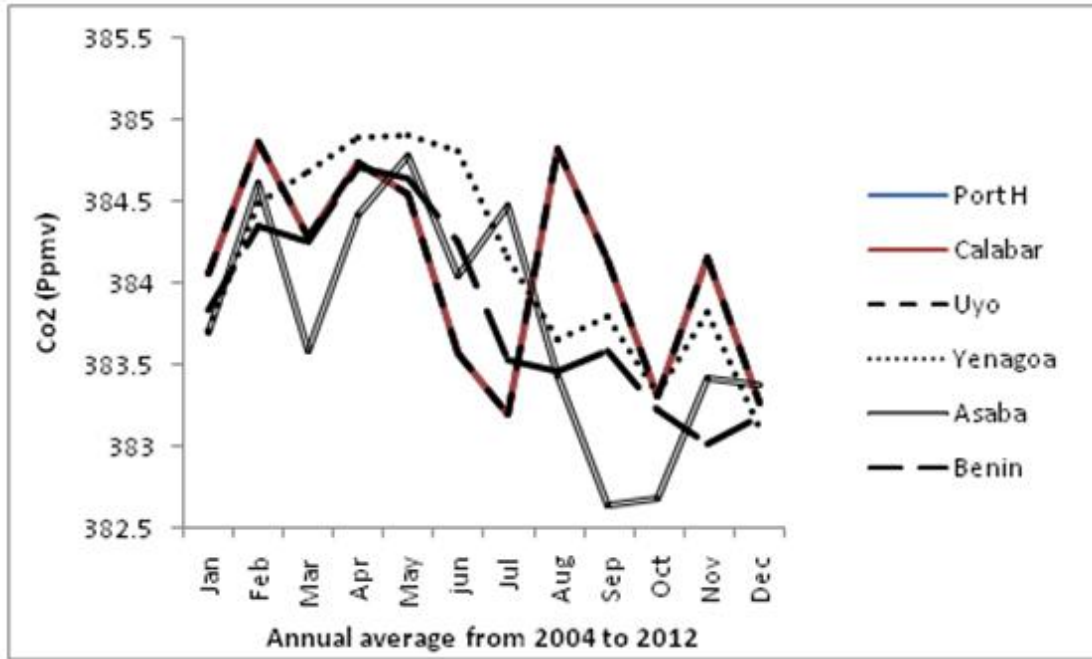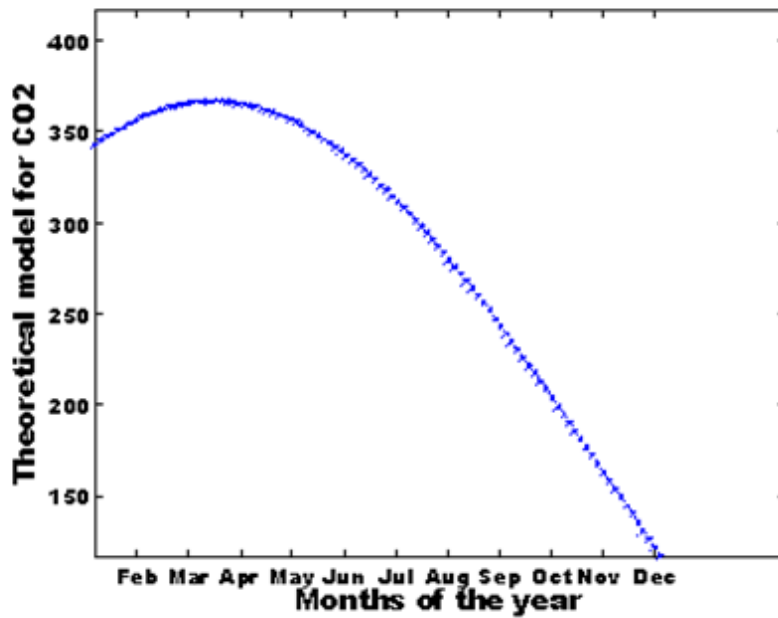
Figure 6: CO₂ satellite analysis from 2004 to 2012

Figure 7: Theoretical model describing the CO₂ pattern and corresponding constants

In January and February there is an increase of the carbon dioxide in the atmosphere in all stations and then in march there is a sharp decrease in Asaba and in port Harcourt, Uyo and calabar followed by Benin with Yenagoa being the most polluted of them all and they all experience a decrease in may, June and then the stations in Port Harcourt, Uyo and calabar experience a drastic increase in CO_2 within July and August while asaba is experiencing a heavy decrease in September and October and they all start to gradually increase in November except Benin which starts increasing in December while others are experiencing steady decrease.
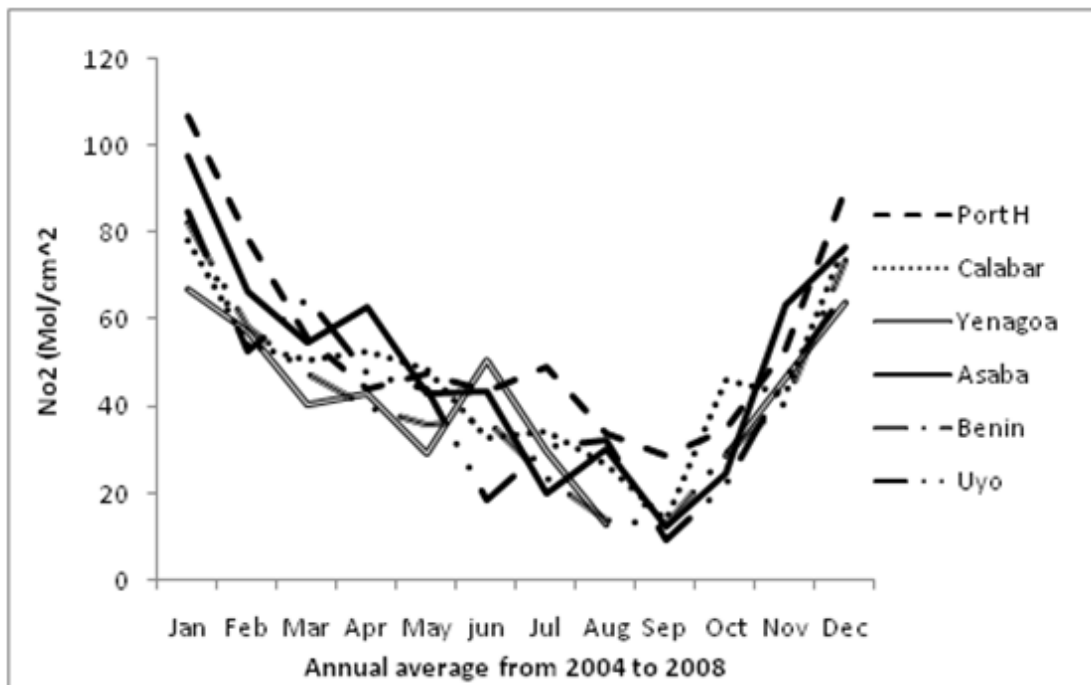

Figure 8: CO_2 satellite analysis from 2004 to 2012

$$\frac{u^2}{\gamma} = 6.95$$

$$u = 0.0005$$

$$\beta = 45$$

$$\frac{u}{k_{NO_2}} = \frac{3}{4}\pi$$

$$\frac{u}{k_{NO_2}} = \frac{1}{4}\pi$$

$$\frac{u}{k_{NO_2}} = \frac{1}{3}\pi$$

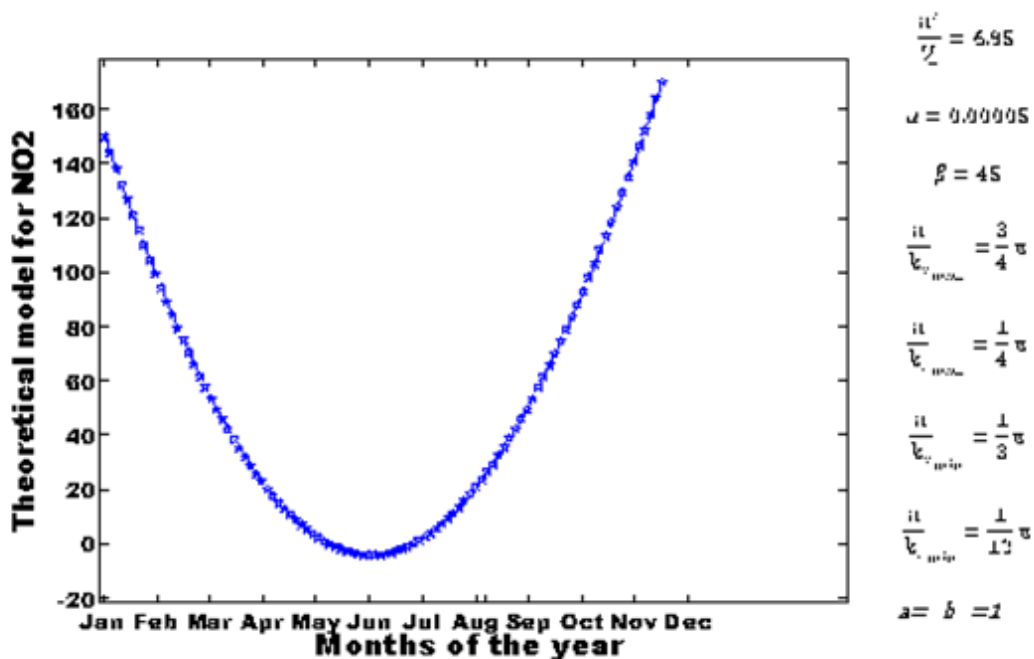$$\frac{u}{k_{NO_2}} = \frac{1}{12}\pi$$

$$a = b = 1$$

Figure 9: Theoretical model describing the NO₂ pattern and corresponding constants

All the stations experience an increase in January with Port Harcourt being the highest followed by Asaba and then Uyo followed by Benin and then calabar with the least being YenYgoa and then in February they all start to decrease from the highest being the Port Harcourt station to the lowest being the Yenagoa station and then in March there is a greater decrease in Yenagoa and then increase in Asaba, Port Harcourt and Calabar and then in April there is a sharp increase in Uyo and Yenegoa while Benin and port Harcourt experience a steady decrease while in April and May we see Yenagoa experiencing an increase as well as calabar while the others maintain a very slow increase and then in June we see the increase in Yenagoa, Asaba and Port Harcourt with decrease in calabar and a drastic decrease in Uyo and in July, August and September they all start to decrease steadily and then in October, November and December they all start to gradually increase until the end of the year with the highest being port Harcourt then Asaba, calabar, Uyo, Benin with the least being Yenagoa
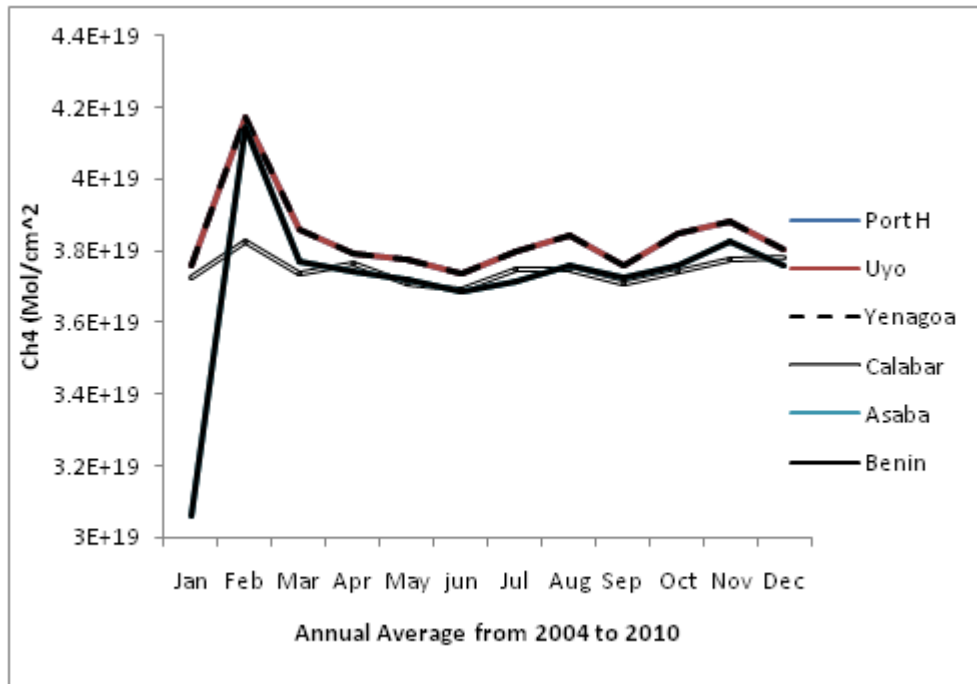
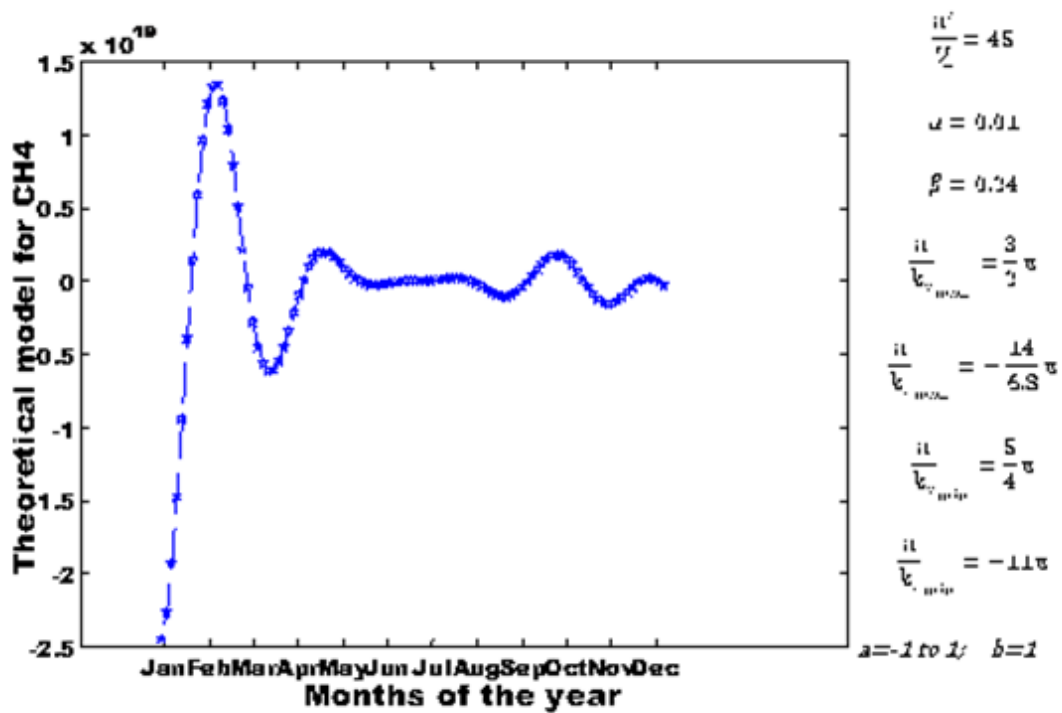**Figure 10: CO₂ satellite analysis from 2004 to 2012**

Figure 11: Theoretical model describing the CH₄ pattern and corresponding constants

In January and February, we saw that the Benin and Asaba station started to increase while the calabar station started to increase gradually while Uyo, Port Harcourt and Yenagoa are their peak of pollution and they all start to decrease in March and April and then they maintain that rate of pollution through may and there is a slight increase in June and July and there is more increase of pollution in August and they all start to decrease in September before picking up again in October and November and then gradually decreasing as the year runs out with the most polluted areas being Port Harcourt, Yenagoa and Uyo.

Table 1: The dispersion parameters describing the individual gas behaviour in the atmosphere

Type	$\dfrac{n^2}{V_x}$	α	β	$\dfrac{n}{k_{y_{max}}}$	$\dfrac{n}{k_{z_{max}}}$	$\dfrac{n}{k_{y_{min}}}$	$\dfrac{n}{k_{z_{min}}}$	$a=b$
CO_2	6.0	5	25	$\dfrac{3}{4}\pi$	$\dfrac{1}{3}\pi$	$\dfrac{1}{4}\pi$	$\dfrac{1}{8}\pi$	1
NO_2	6.95	0.00005	45	$\dfrac{3}{4}\pi$	$\dfrac{1}{4}\pi$	$\dfrac{1}{3}\pi$	$\dfrac{1}{12}\pi$	1
SO_2	-0.005	0.05	0.34	$\dfrac{5}{4}\pi$	$-\dfrac{14}{4}\pi$	$\dfrac{3}{2}\pi$	$-\dfrac{17}{2}\pi$	1
CH_4	45	0.01	0.24	$\dfrac{3}{2}\pi$	$-\dfrac{14}{6.8}\pi$	$\dfrac{5}{4}\pi$	-11π	$a \neq b$

As seen in table 1, SO2 have the highest speed at the Niger-delta atmosphere. Its angular displacements are very small. Hence may not spread like other gases. It has the tendency to go downward whenever precipitation is high. Therefore if gas flaring continues, SO2 has the potential of creating greater damage in the Niger- Delta region. NO2 and CO2 have almost the same characteristics except that its horizontal angular displacement is very small. CH4 have the lowest speed in the atmosphere of the Niger-Delta. It diffuses into the atmosphere in a slow but steady manner. Unlike SO2, its volume in the atmosphere is not affected by much precipitation. Therefore may be eliminated only after its expiration of its life-time. The glaring peaks noticed in January and February shows the tendency of its mean equilibrium to rise above its current state. SO2 and CH4 have often stable and shallow atmospheric boundary layer at night-causing the mixing ratio to build up in a thin layer near the surface. During the day, the boundary layer is often convective and deep-causing it to dilute over large vertical extent. It has the tendency to go downward whenever precipitation is high. Therefore if gas flaring continues, SO2 has the potential of creating greater damage in the Niger- Delta region. NO2 and CO2 has almost the same characteristics except that its horizontal angular displacement is very small. Against the rectifier effect theory noticed for CO2 (Vincent et al., 2008), the Niger-Delta region do not observe the asymmetric mixing ratio of the rectified CO2.

4 Conclusion

The movement of atmospheric pollution across large land mass is of concern to mankind. Therefore the struggle against the emission of greenhouse gases or aerosols into our environment should not be underestimated. Policies relating to climate protection must be taken into account as can be seen in the mathematical projection of the four gases considered. The Niger-Delta region is therefore the trigger point for pollution of the entire land mass via the moist south wind speed from the coastline. Therefore strict compliance to air-quality management would not salvage the people living in the Niger-Delta but the entire life-form around its vicinity.

References

[1] Emetere, and M.L Akinyemi, Modeling Of Generic Air Pollution Dispersion Analysis From Cement Factory. Analele Universitatii din Oradea–Seria Geografie **231123-628**, pp181-189, 2013.

[2] Emetere,Moses E., Modeling Of Particulate Radionuclide Dispersion And Deposition From A Cement Factory. Annals of Environmental Science,**7 (6),** pp71-77, 2013.

[3] Emetere, M. E., Theoretical Forecast of the Health Implications of Citing Nuclear Power Plant in Nigeria, Journal of Nuclear and Particle Physics, **4 (3)**, pp87-93,2014

[4] Watts M. (2001). Petroleum violence: communities, extraction and political ecology of a mythic commodity.189-212pp. Cornell University Press

[5] NASA,http://www.nasa.gov/audience/foreducators/9-12/features/giovanni-an-easier-way.html 2009

[6] Ana, G.R. and E.E. Sridhar, Industrial Emissions and Health Hazards among selected factoryworkers at Eleme, Nigeria. J. Env. Heal. Res., **l9 (1)**, pp43-51, 2009.

[7] Tawari C.C. and J.F.N. Abowei, Air Pollution in the Niger Delta Area of Nigeria, International Journal of Fisheries and Aquatic Sciences **1 (2),** 94-117, 2012

[8] Dinesh K. S., Modelling Cyber-security. International Journal of Applied Physics and Mathematics, **2 (5)**, pp312-315, 2012

[9] Uno EU, Emetere M E. Analysing the Impact of Soil Parameters on the Sensible Heat Flux Using Simulated Temperature Curve Model. International Journal of Physics & Research, **2**, pp1-9, 2012

[10] Uno EU, Emetere ME, Eneh C D. Simulated Analysis of soil heat flux using temperature deviation model. Science Journal of Physics, **2012**, pp1-9, 2012

[11]   Lovejoy ER, Curtius J, Froyd KD. Atmospheric ion-induced nucleation of sulphuric acid and water, Journal of Geophysical Research, 2004, 109: D08204.

[12]   de Gouw JA, Warneke C, Stohl A, Wollny AG, Brock CA, Cooper OR, Holloway JS, Trainer M. Volatile organic compounds composition of merged and aged forest fire plumes from Alaska and western Canada, *Journal of Geophysical Research*, 2006,111: D10303.